Indian J. Phys. **75A** (4), 327-333 (2001)

IJP A
— an international journal

Collective excitations in aligned carbon nanotube superlattices

P Longe
Institut de Physique B5, Université de Liège, Sart-Tilman, B-4000 Liège, Belgium
and
S M Bose*
Department of Physics and Atmospheric Science, Drexel University,
Philadelphia, Pennsylvania 19104, USA

E-mail : bose@drexel.edu

Abstract : The collective electronic excitation (plasmon) modes of aligned carbon nanotube superlattices have been calculated The nanotubes are described by two-dimensional electron gases (2DEG) confined on hollow cylindrical surfaces which are regularly aligned in a plane forming the 2D superlattice, or which form a hexagonal closed-pack structure producing the 3D superlattice The series of modes obtained in the random phase approximation can be presented as combination of three contributions : (i) a one-tubule contribution, (ii) a uniform 2D or 3D bulk contribution, and (iii) a contribution related to the lattice structure. For plasmon wavelengths small compared to the distance a between axes, these modes tend to be those of individual tubules, *i.e.* the one-tubule contribution is dominant for $aq >> 1$ (q = momentum). For large wavelengths, however, they tend to those of the 2D or 3D uniform electron gas, *i.e* the bulk contributions dominate for $aq << 1$. The lattice contribution to plasmon frequency is most significant at intermediate wavelengths

Keywords . Electronic properties, aligned carbon nanotubes

PACS Nos. : 85.35.kt, 73.22 Lp, 73.21 Col

1. Introduction

Ever since the discovery of carbon (graphitic) nanotubes [1,2], it was realized that they might have useful applications in nanoscale engineering and electronics. As their properties were being studied by various investigators, it was apparent that their characterization and commercial applications would be facilitated if aligned samples of carbon nanotubes could be produced in bulk quantities.

Ajayan *et al* [3] were the first to produce aligned arrays of carbon nanotubes by cutting polymer-resin nanotube composites. However, because of the presence of the resin-matrix and because the degree of alignment were dependent on the thickness of the sample, these aligned nanotubes were not ideal for study of their properties. To produce aligned nanotubes, de Heer *et al* [4] first created a suspension of nanotubes in ethanol and then passed the suspension through a 0.2 μm-pore ceramic filter which produced a black deposit on the filter. They then transferred the deposited material onto a plastic surface (teflon or derlin) and then rubbed the surface with teflon or aluminum foil which produced an aligned and densely packed nanotube film. However, this method apparently produces nanotubes of different sizes some of which also stick together thus affecting their properties. Single-walled aligned bundle of nanotubes were then produced by Thess *et al* [5] by metal catalyzed laser ablation of graphite. More recently, Li *et al* [6] have reported large-scale synthesis of aligned carbon nanotubes by a chemical vapor deposition technique catalyzed by iron nanoparticles embedded in mesoporous silica. It was then pointed out by Terrones *et al* [7] that the commonly used methods to generate nanotubes have the drawback that they also form polyhedral particles and that the nanotubes are variable in size. By using a laser etching method they achieved controlled production of aligned nanotube bundles of length up to 50 μm and of fairly uniform diameters (30-50 nm) and uncontaminated by polyhedral particles.

These discoveries have led to the study of various properties of the aligned carbon nanotubes. De Heer *et al* [4] were the first to measure the optical properties (frequency dependent dielectric function) and electronic properties (temperature dependent resistivity) on the aligned nanotubes they produced. Using an effective medium theory Garcia-Vidal *et al* [8] calculated the real and imaginary parts of the dielectric function and found good

* Corresponding Author

agreement with de Heer *et al.*'s experimental data. Lee *et al* [9] on the other hand produced K and Br doped single-walled carbon nanotube bundles by vapor phase reactions and measured their conductivity enhancement due to doping. In another paper de Heer *et al* [10] reported that aligned carbon nanotubes have excellent field emission properties and they made a high-intensity electron gun based on their field emission properties. Baumgartner *et al* [11] studied the magnetic properties of aligned nanotubes and showed that the Hall coefficient (R_H) is positive in a wide temperature range indicating prominence of hole conduction. They also reported that the magneto-resistance ($\Delta\rho_m / \rho_m$) is negative at low fields which suggest there may be noncoherent transport between nanotubes. Chauvet *et al* [12] carried out measurements of static susceptibility and electron-spin resonance which show substantial anisotropic behavior in the magnetic properties of the aligned nanotubes.

In this paper, we undertake a theoretical study of the electronic properties of the aligned nanotube samples and in particular calculate their collective excitation (plasmon) modes by using and extending a model previously developed by the present authors for the study of a layered two-dimensional electron gas (2DEG) [13] and coaxial nanotubes [14]. The electrons are assumed to be distributed on the surfaces of the hollow nanotubes forming cylindrical 2DEGs. These nanotubes are either regularly aligned in a plane forming a two-dimensional superlattice (2DSL), or they are arranged in a hexagonal closed pack structure forming a three-dimensional superlattice (3DSL). Taking into account both the intra- and inter-tubule electronic Coulomb interaction we carried out a many-body calculation of the dielectric function for both superlattices. The collective excitation (plasmon) modes are then obtained by imposing the condition of cancellation of the dielectric function. In two recent papers Lin *et al* [15,16] have calculated the electron energy loss spectra and plasmon excitations in carbon nanotube bundles arranged in a three dimensional lattice. As will be seen later, our calculation differs from theirs in several significant respects and the results obtained are different in details.

The plasmon frequencies obtained for the 2DSL and 3DSL are presented in Sections 3 and 4, respectively, along with the plasmon frequencies of a single nanotube and of a uniform 2DEG or 3DEG for the purpose of comparison.

2. The multilayered system

Before embarking on the calculation of the 2D and 3D nanotube superlattice (SL) excitation modes we briefly review the results of multilayered planar 2DEGs [13] and of the single tubule [14]. This theory will then be extended to the aligned nanotubes in the following sections. The calculation is done in the random phase approximation, the validity of which has been discussed by the present authors in Ref. [14]. The plasmon dispersion relations are obtained by the usual method based on the cancellation of the real part of the (complex) dielectric function. For a uniform electron gas of dimensionality d, one has

$$\mathrm{Re}\,\varepsilon(q,\omega_p) = 1 + v_0(q)\,\Pi_d(q,\omega_p) = 0\,, \tag{1}$$

where momentum q is a d-vector, $v_0(q)$ is the Coulomb potential and $\Pi_d(q,\omega)$ is the electron-hole propagator. If q does not exceed the Fermi momentum k_F, one can write

$$\Pi_d(q,\omega) = -\rho_d\, q^2 / m\omega^2\,, \tag{2}$$

where ρ_d is the electron density and m is the usual (bare) electron mass.

The following table gives the expressions of $v_0(q)$ and ρ_d for $d = 3, 2$, and 1. The last column gives the plasmon (squared) frequency deduced from (1).

	$v_0(q)$	ρ_d	ω_p^2	
3	$4\pi e^2 / q^2$	$k_F^3 / 3\pi^2$	$4\pi e^2 \rho_3 / m$	(3a)
2	$2\pi e^2 / q$	$k_F^2 / 3\pi$	$(2\pi e^2 \rho_2 / m)q$	(3b)
1	$2e^2 K_0(qr_0)$	$2k_F / \pi$	$(2e^2 \rho_1 / m)q^2 K_0(qr_0)$	(3c)

Note that, in the last line of this table, the 1DEG is in fact a 2DEG confined on a cylindrical surface of radius r_0, the modified Bessel function ($K_0(qr_0)$ being divergent for $r_0 \to 0$. More precisely for such a tubular electron gas, one has

$$v_0(q) = 4\pi e^2 r_0 I_0(qr_0)\, K_0(qr_0), \tag{4}$$

where the modified Bessel functions I_0 and K_0 behave as

$$I_0(qr_0) \approx 1, \tag{5}$$

$$K_0(qr_0) \approx -\gamma + \ln(2 / qr_0) = \ln(1.123 / qr_0),$$

for small arguments ($\gamma = 0.577$ is the Euler constant). This yields

$$\omega_p^2 = (\rho_2 q^2 / m) 4\pi e^2 r_0 I_0 K_0$$

$$\approx (2e^2 \rho_1 / m) q^2 K_0(qr_0),$$

with $\rho_1 = 2\pi r_0 \rho_2$, as given in eqs. (2) and (3c).

As a prototype for a superlattice, let us consider multilayered electron gas. This system is a deck of parallel 2DEG (layers) separated by a distance a. To treat this system, the 2D potential $v_0(q) = 2\pi e^2 / q$ is extended outside the 2DEG by multiplying it with the factor $e^{-q|z|}$ related to the 3rd dimension z perpendicular to the layers. Eq. (1) then takes the form [13]

$$1 + v_0(q)\, f(q,\kappa)\, \Pi_2(q,\omega) = 0, \tag{6}$$

where $f(q,\kappa)$ is a geometrical factor given by

$$f(q,\kappa) = \sum_{\Delta n=-\infty}^{\infty} \exp\left(i\kappa\Delta n - |\Delta n|aq\right)$$

$$= \sinh aq / (\cosh aq - \cos \kappa). \quad (7)$$

This factor is the Fourier transform of the z-part of the potential. It is given by

$$e^{-q|\Delta z|} = e^{-aq|\Delta n|} = \frac{1}{2\pi} \int_{-\pi}^{\pi} d\kappa \, f(\kappa, q) e^{-i\kappa \Delta n},$$

where the n's are integers labeling the consecutive layers of the system, and where $\kappa = aq_z$ can be related to a 3rd component q_z perpendicular to the 2D-vector q. From (6), one obtains the plasmon dispersion relation [13]

$$\omega_p^2 = (2\pi e^2 \rho_2 / m) q \, f(\kappa, q). \quad (8)$$

Let us mention several special features of this theory. The 2DEG plasmon dispersion relation $\omega_p \propto \sqrt{q}$, given in (3b), is represented by a curve in (ω, q)-space. For the multilayered system, this curve is replaced by a band which extends between two limits : an *acoustic limit* $\omega_p \propto q$, corresponding to $\kappa = \pm\pi$, and an *optical limit* $\omega_p \propto$ *constant*, corresponding to $\kappa = 0$. Indeed, one has $f(\pm\pi, q) = \tanh(aq/2) \approx aq/2$, and from (6) this gives $\omega_p \propto q$. On the other hand, one has $f(q, 0) = \coth(aq/2) \approx 2/aq$, giving $\omega_p \approx$ *constant*. Moreover if the whole 3D-vector $Q \equiv (q, q_z)$ is assumed to be small compared to $1/a$, one has $f(q, aq_z) \approx 2q / aQ^2$. For this *small momentum limit*, the plasmon frequency becomes

$$\omega_p^2 = (4\pi e^2 / m)(\rho_2 / a)(q / Q)^2 = (4\pi e^2 \rho_3 / m) \cos^2 \theta.$$

This is the well known expression of the bulk plasmon frequency (for an electron density $\rho_3 = \rho_2 / a$) where θ is the angle between vector Q and the layer planes. Finally let us note that $f(q, \kappa) \sim 1$ for $a \to \infty$, and expression (6) then goes back to the plasmon frequency of a single 2DEG. This is the *one-layer limit*, corresponding to a negligible layer-layer interaction.

The above discussion shows that the plasmon (squared) frequency of a multilayered system can be considered as the sum of three terms : (i) a *one-layer* contribution, equivalent to the plasmon frequency of a single 2DEG,

$$\left[\omega_{p,1lay}(q)\right]^2 = (2\pi e^2 \rho_2 / m) q,$$

(ii) a *uniform bulk* contribution (equivalent to a 3D plasmon)

$$\left[\omega_{p,uni3}(q, q_z)\right]^2 = (4\pi e^2 / m)(\rho_2 / a)(q / Q)^2;$$

and (iii) a 3rd contribution

$$\left[\omega_{p,lat}(q, q_z)\right]^2 = (2\pi e^2 \rho_2 / m) q \left[f(q, \kappa) - 1 - 2q / aQ^2\right]$$

which is essentially due to the *lattice structure*. The one-layer contribution is dominant for $aQ >> 1$. On the contrary, the bulk contribution will dominate for $aQ << 1$.

These results are presented here because they form the framework in which we will investigate the collective modes of the nanotube superlattices.

3. The two-dimensional nanotube superlattice

A 2DSL can be treated as a system of parallel 1DEGs aligned in a plane and separated by a distance a. This system is not formally different from the above multilayered electron gas, the periodicity of both systems being one-dimensional. An equation similar to (6) can be set up in the form

$$1 + 2e^2 F(q, \kappa) \Pi_1(q, \omega) = 0 \quad (9)$$

with

$$F(q, \kappa) = \sum_{n=-\infty}^{\infty} e^{i\kappa \cdot n} K_0(qa\Delta n). \quad (10)$$

Here, the ID potential (4) has been extended to interactions between electrons located on *different* tubules. It has been replaced by

$$v_0(q, r) = 4\pi e^2 r_0 I_0(qr_0) K_0(qr) \quad \text{with } r \geq r_0. \quad (11)$$

This is the interaction between an electron located on a tubule, and another electron located at a distance r from the axis of the tubule. It is the Coulomb interaction expressed in cylindrical coordinates, where only the longitudinal part is considered. The azimuthal part may be important as in the study of systems like the coaxial tubules investigated in Ref. [14]. But here, for the collective modes of a 2DSL, this part can be disregarded. As in (5), it is also assumed that $I_0(qr_0) \approx 1$. Moreover, since only the linear electron density is important, 1D expressions like $\rho_1 = 2\pi r_0 \rho_2$ and $\Pi_1(q, \omega) = 2\pi r_0 \Pi_2(q, \omega)$ are introduced, in agreement with (2) and (3) (a factor $2\pi r_0$ is removed from the potential and re-introduced into the propagator $\Pi_1 = 2\pi r_0 \Pi_2$). As a last step, $v_0(q)$ is introduced into (10) in the form

$$v_0(q) = 2e^2 K_0(qr_{nn'}), \quad (12)$$

where $r_{nn'}$ can be identified with the distance between the axes of tubules n and n'. However, for electrons located on the same tubule ($n = n'$), K_0 is divergent, and the original argument qr_0 has to be kept in the term $\Delta n = 0$. Hence (10) is finally written as

$$F(q, \kappa) = K_0(qr_0) + \sum_{\Delta n = -\infty}^{\infty} e^{i\kappa \Delta n} K_0(qa|\Delta n|) - K_0(0) \Big|. \quad (13)$$

The first term is a one-tubule term, corresponding to the one-layer term for the multilayered system. Its contribution to ω_p^2 is the same as given in (3) for $d = 1$. The second term (in brackets) yields the uniform 2DEG contribution together with the lattice contribution.

This can be shown explicitly by using the Fourier transform of $K_0(q|x|)$, *i.e.*

$$K_0(q|x|) = \frac{1}{2\pi}\int_{-\infty}^{\infty} dq_\perp\, e^{iq_\perp x} p/\sqrt{(q_\perp^2+q^2)}, \qquad (14)$$

where $q_\perp$ is a second component transforming the 1D momentum vector q (along the tubules) into the 2D vector $Q \equiv (q, q_\perp)$ within the 2DSL plane. This component can be written as

$$q_\perp = (2\pi s+\kappa)/a \qquad (15)$$

with $-\pi < \kappa < \pi$, s being an integer (lattice vector). By writing (14) as

$$K_0(qa|n|) = \frac{1}{2\pi}\sum\int_{-\pi}^{\pi} d\kappa' e^{in\kappa'} S_1(2\pi s+\kappa') \qquad (16)$$

with

$$S_1(2\pi s+\kappa) = \pi\left[(2\pi s+\kappa)^2 + a^2q^2\right]^{-1/2},$$

eq. (13) takes the form

$$F(q,\kappa) = K_0(qr_0) + \frac{1}{2\pi}\sum_{s=-\infty}\int_{-\pi}^{\pi} d\kappa'\left[S_1(2\pi s+\kappa) - S_1(2\pi s+\kappa')\right]. \qquad (17)$$

Two terms of this expression diverge for small (q,κ) : the first term $K_0(qr_0)$ and the term $s = 0$ in the sum, this latter term yielding $\ln(aq) + \pi/\sqrt{(\kappa^2+a^2q^2)}$.

The above discussion shows that three contributions to ω_p^2 come out of (17) : (i) a *one-tubule* term equivalent to the contribution of single 1DEG's,

$$F_{1tub}(q,\kappa) = K_0(qr_0),$$

substitution of this in (9) gives

$$\left[\omega_{p,1tub}(q)\right]^2 = (2e^1\rho_1/m)q^2K_0(qr_0)$$

as in (3c) ;

(ii) a *uniform layer* contribution, equivalent to a 2DEG contribution,

$$F_{uni2}(q,\kappa) = \pi\left[\kappa^2+a^2q^2\right]^{-1/2} = \pi/aQ$$

giving

$$\left[\omega_{p,uni2}(q,\theta)\right]^2 = (2\pi e^2/m)(\rho_1/a)q\cos\theta$$

where $\theta = \cos^{-1}(q/Q)$ is the angle between Q and the tubule axes – see (3b); (iii) a third contribution, essentially due to the presence of a *lattice structure*, which can be written as

$$F_{lat}(q,\kappa) = 2\sum_{n=1}^{\infty}\cos\kappa n\, K_0(qan) - \pi/\sqrt{(\kappa^2+a^2q^2)}.$$

For small (q,κ), this expression has a $\ln(aq)$ behavior however, ω_p^2 obtained by using this term will be finite Substitution of (13) in (9) yields the effective plasmon frequency $\omega_{p,eff}(q,\kappa)$.

The curves representing $\omega_{p,eff}$, together with $\omega_{p,1tub}$ and $\omega_{p,uni2}$ are plotted in Figure 1. In all our calculations, we have chosen the following data : as in Ref. [14] we consider tubules with an electron density $\rho_s = 0.38\text{Å}^{-2}$ and a radius $r_0 = 3.39$Å [*i.e.* $B(2, 1)5$ tubules]. This yields $\rho_1 = 2\pi r_0\rho_s = 8.13\text{Å}^{-1}$ for the linear density along the tubules. Moreover, we choose $a = 3r_0 = 10.17$ Å for the intertubule separation (distance between two adjacent tubules), a value close to the one used by Tersoff and Ruoff [17] for a nanotube lattice.

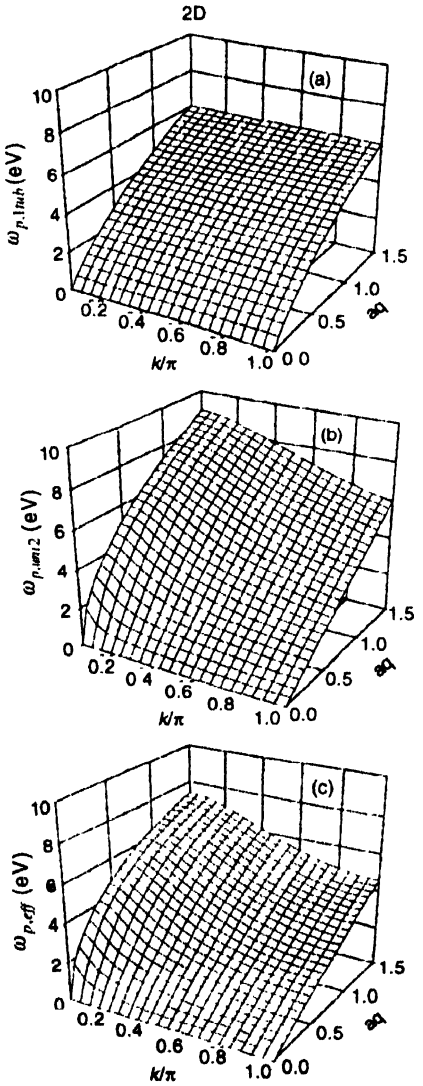

Figure 1. Three-dimensional contour plots of the plasmon frequencies $\omega_{p,1tub}$(a), $\omega_{p,uni2}$ (b) and $\omega_{p,eff}$ (c) of the 2D system as functions of and κ. These plots clearly show that the plasmon frequencies can both b optical and acoustic at different values of the wave vector components

In Figure 1 (a), (b) and (c), we plot the contours of plasmon frequencies $\omega_{p,1tub}$, $\omega_{p,uni2}$ and $\omega_{p,eff}$, respectively, a

functions of the momentum components q and κ. Figure 1 (a) shows that the one tubule frequency is independent of κ because of the quasi-one-dimensional nature of the tubules. In the quasi-uniform two-dimensional limit (Figure 1 (b)), the plasmon frequency develops both q and κ dependence and as can be seen for each value of q, the frequency is the highest for $\kappa = 0$ and the lowest for $\kappa = \pi$. This is expected as $\kappa = 0$ provides the easy direction for electrons to participate in the oscillation (symmetric modes) whereas $\kappa = \pi$ corresponds to the antisymmetric oscillations of the electrons in the nanotube superlattice. For small q, the plasmon frequency has a linear (acoustical) behavior for nonvanishing κ. For vanishing κ, however, this frequency has a $\sqrt{q}$ behavior. Similar behavior is also observed for the effective plasmon frequency $\omega_{p,eff}$ as shown in Figure 1 (c) which includes the contribution of the lattice structure of the 2D lattice. A comparison of Figures 1 (b) and 1 (c) indicates that the lattice has the effect of diminishing the plasmon frequency. Again this is expected since when the electrons are arranged in a lattice, they lose some freedom to oscillate because of the constraints imposed by the lattice structure not present in the 2DEG. It is interesting to note that values of $\omega_{p,eff}$ are intermediate between those of 2DEG and one tubule. It is evident that $\omega_{p,eff}$ converges to $\omega_{p,uni2}$ for small values of aq whereas it approaches $\omega_{p,1tub}$ for large values q as is expected from physical considerations.

4. The three-dimensional nanotube superlattice

In the 3DSL, the tubules are stacked against each other forming a hexagonal closed packed structure. As for the 2DSL, this system is treated as a set of aligned 1DEG's separated by a distance a. A cross section perpendicular to the tubule axes appears as a close-packed triangular 2D Bravais lattice with a as a lattice constant (see lower part of Figure 2). For this system expressions similar to (9) and (10) can be written. The main change is that here κ is a 2D-vector. Eq. (13) is then modified into

$$F(q,\kappa) = K_0(qr_0) + \left[\sum_{n_1=-\infty}^{\infty} \sum_{n_2=-\infty}^{\infty} e^{i(\kappa_1 n_1 + \kappa_2 n_2)} K_0(qa\,|n|) - K_\ell(0) \right] \tag{18}$$

where (n_1, n_2) and (κ_1, κ_2) are 2D-vectors defined in the direct lattice and in the reciprocal lattice, respectively. More precisely, in the direct lattice, one has

$$n = (n_1 \boldsymbol{a}_1 + n_2 \boldsymbol{a}_2)/a,$$

where $|\boldsymbol{a}_1| = |\boldsymbol{a}_2| = a$, and $|\boldsymbol{a}_1 \times \boldsymbol{a}_2| = a^2 \sin 60^0$, n_1 and n_2 being integers (lattice vector). In the reciprocal lattice, the momentum component $\boldsymbol{q}_\perp$, perpendicular to the tubule axes, is defined as

$$\boldsymbol{q}_\perp = q_1 \boldsymbol{b}_1 + q_2 \boldsymbol{b}_2$$

with $\boldsymbol{b}_1 = \boldsymbol{a}_2 \times \boldsymbol{u}/|\boldsymbol{a}_1 \times \boldsymbol{a}_2|$ and $\boldsymbol{b}_2 = \boldsymbol{u} \times \boldsymbol{a}_1/|\boldsymbol{a}_1 \times \boldsymbol{a}_2|$, $\boldsymbol{u}$ being the unit vector along the tubule axes ; hence $a_i\, b_j = \delta_{ij}$. The components are then written as

$$q_i = 2\pi s_i + \kappa_i,$$

where (s_1, s_2) are integers (reciprocal lattice vector), and where $-\pi < (\kappa_1, \kappa_2) < \pi$.

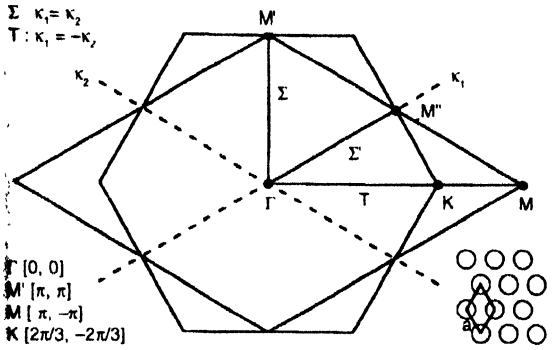

Figure 2. The three-dimensional tubule superlattice seen in cross section, appears as a triangular close-packed Bravais lattice (lower right part of the figure) This figure depicts the primitive cell in the reciprocal 2D lattice which may be a losange (reported to the axes κ_1 and κ_2), or a hexagonal Brillouin zone The plasmon frequency ω_p has been calculated for momentum κ ranging along two symmetry directions (i) Direction T, defined by $\kappa \equiv \kappa_1 = \kappa_2$, with the symmetry points $\Gamma[\kappa = 0]$, and $M'[\kappa = \pi]$; (ii) direction Σ, defined by $\kappa \equiv \kappa_1 = -\kappa_2$, with the symmetry points $\Gamma[\kappa = 0]$, $K[\kappa = 2\pi/3]$ and $M[\kappa = \pi]$.

The treatment of (18) for the 3DSL is quite similar to the treatment of (13) for the 2DSL. Here a 2D Fourier transform of $K_0(q\,|\,x\,|)$ is introduced, *i.e.*

$$K_0(q\,|\,x\,|) = \frac{1}{(2\pi)^2} \iint d^2 q_\perp\, e^{i q_\perp \cdot r}\, 2\pi/(q_\perp^2 + q^2) \tag{19}$$

giving

$$K_0(qa\,|\,\boldsymbol{n}\,|) = \frac{1}{(2\pi)^2} \sum\sum \int_{-\pi}^{\pi} d\kappa_1' \int_{-\pi}^{\pi} d\kappa_2' e^{i(\kappa_1 n_1 + \kappa_2 n_2)} S_2(2\pi s_i + \kappa_i') \tag{20}$$

with

$$S_2(p_i) = (\pi\sqrt{3})/\left[p_1^2 + p_2^2 - p_1 p_2 + 3a^2 q^2/4\right].$$

Hence

$$F(q,\kappa) = K_0(qr_0) + \frac{1}{(2\pi)^2} \sum_{s_1} \sum_{s_2} \int_{-\pi}^{\pi} d\kappa_1' \int_{-\pi}^{\pi} d\kappa_2' \left[S_2(2\pi s_i + \kappa_i) - S_2(2\pi s_i + \kappa_i')\right].$$

As in (17), two terms diverge for small (q,κ) : the first term $K_0(qr_0)$, and the term $s_1 = s_2 = 0$ in the sum. This latter term yields $\ln(aq) + (4\pi/\sqrt{3a^2})/(q^2 + q_\perp^2)$ with

$$q_\perp^2 = (4/3a^2)(\kappa_1^2 + \kappa_2^2 - \kappa_1\kappa_2).$$

As for the 2DSL, $F(q,\kappa)$ given by (21), yields three types of contributions to ω_p^2 :

(i) a *one-tubule* contribution related to the term $K_0(qr_0)$, and giving $\left[\omega_{p,1tub}(q)\right]^2$ as before ;

(ii) a *uniform bulk* contribution coming from $(4\pi/\sqrt{3a^2})/(q^2+q_\perp^2)$, and giving

$$\left[\omega_{p,uni3}(q,\theta)\right]^2 = (4\pi e^2\rho_3/m)\cos^2\theta,$$

where $\theta = \cos^{-1}(q/Q)$ is the angle between the 3D-momentum $Q \equiv (q, q_\perp)$ and the tubule axes [see (3a)]. Note that a 3D-density $\rho_3 = \rho_1/(a^2 \sin 60^0)$ has been introduced in this latter expression ;

(iii) a 3rd contribution, essentially due to the presence of a *lattice structure*, which can be written as

$$F_{latt}(q,\kappa) = \sum_{n_1\neq 0}\sum_{n_2\neq 0} e^{i(\kappa_1 n_1+\kappa_2 n_2)} K_0(q_a|n|)$$

$$-(4\pi/3a^2)/(q^2+q_\perp^2).$$

Like the 2DSL case, for small (q,κ) this expression also has a $\ln(aq)$ behavior, however, ω_p^2 obtained by using this term would also be finite. The effective plasmon frequency for the 3DSL, $\omega_{p,eff}(q,\kappa)$ can be obtained by substituting (21) in (9).

The plasmon frequencies have been calculated for momentum κ ranging along two symmetry directions : (i) direction T, defined by $\kappa \equiv \kappa_1 = \kappa_2$, with the symmetry points $\Gamma[\kappa=0]$, and $M'[\kappa=\pi]$; (ii) direction Σ, defined by $\kappa \equiv \kappa_1 = -\kappa_2$, with the symmetry points $\Gamma[\kappa=0]$, $K[\kappa=2\pi/3]$ and $M[\kappa=\pi]$. This geometry is depicted in Figure 2.

The contours of the plasmon frequencies $\omega_{p,1tub}$, $\omega_{p,uni3}$ and $\omega_{p,eff}(q,\kappa)$ as functions of q and for two different directions of the Brillouin zone $\Sigma \equiv \Gamma M$ and $T \equiv \Gamma KM$ are plotted in Figure 3(a), (b) and (c), respectively. As noted before, the single tubule result (Figure 3(a)) is independent of κ since electrons have been allowed to have only quasi-one-dimensional oscillations. As in the case of a quasi-2D uniform and 2DSL (Figures 1(b) and (c)), the quasi-3D uniform and 3DSL (Figures 3(b) and (c)) have maximum plasmon frequency at the Γ point (corresponding to $\kappa = 0$) for all values of q. This corresponds to the true optical nature of the plasmon frequency. In particular, the frequency related to $\kappa = 0$ tends to the classical bulk plasmon frequency for $q \sim 0$. As we move away from the Γ point, the plasmon frequency diminishes for all values of q. Note that it demonstrates quasi-acoustic behavior near $q = 0$ for all values of κ except for the Γ point. The plasmon frequencies presented by Lin *et al* [15, 16] seem to be optical in nature for all directions. This may be because they do not carry out a proper lattice sum for a hexagonal closed packed lattice. The lattice structure diminishes the plasmon frequency for exactly the same reason as discussed in the case of 2DSL. In Figure 3 (c) (in the presence of the lattice), the plasmon frequency goes up between K and M points, while it continues to go down in Figure 3 (b). This is due to the equivalence of the lattice points M and M' and M'' in the periodic zone scheme (see Figure 2). In the limit of large aq, $\omega_{p,eff}$ approaches the result corresponding to a single tubule result, whereas for small aq, $\omega_{p,eff}$ approaches values of $\omega_{p,uni3}$.

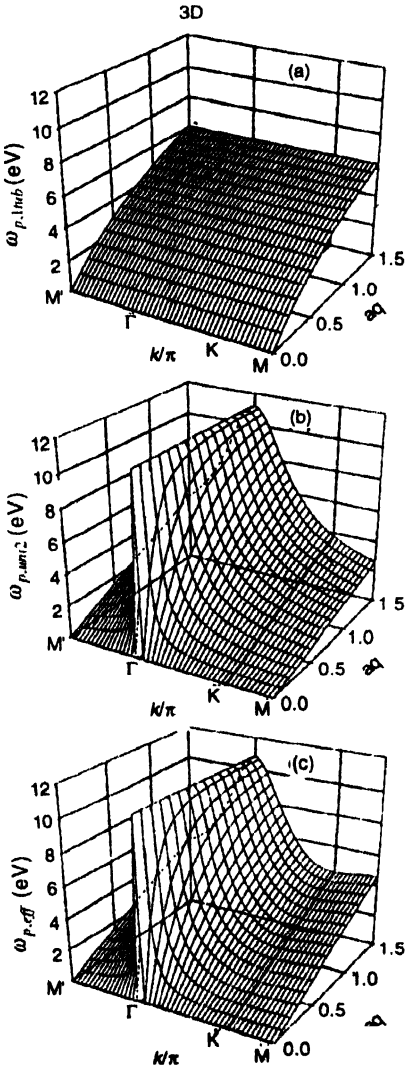

Figure 3. Three-dimensional contour plots of the plasmon frequencies $\omega_{p,1tub}$(a), $\omega_{p,uni3}$ (b) and $\omega_{p,eff}$ (c) of the 3D system as functions of q and κ. Two different symmetry directions Σ and T as described in Figure 2 have been selected for these plots. The frequencies corresponding to the K point (see Figure 2) are those along the thick line, and the frequencies corresponding to Γ are on the crest of the plot. These plots clearly show that the plasmon frequency is fully optical at Γ point and it can have acoustic behavior at other κ values for small q.

5. Discussion

In this paper we have carried out a calculation of the collective electronic excitation modes (plasmon dispersion) of carbon

nanotubes aligned either in a plane forming a 2DSL or in a hexagonal closed packed structure in three-dimension giving rise to a 3DSL. The dielectric function has been formulated in the many-body formulation using the random phase approximation. The plasmon dispersion is obtained from the zeros of the dielectric function.

The effective plasmon frequencies thus obtained along with the plasmon frequencies of a single nanotube and of a uniform 2DEG or 3DEG have been plotted in Figure 1 for the 2DSL and in Figure 3 for the 3DSL. It is seen that the direction along the axes of the nanotubes is the "easy direction" for the excitations of the plasmons and thus for any q, the maximum occurs when $\lambda = 0$ for the 2D system and at Γ-point for the 3D system. At these points, the plasmon frequency is truly optical for all values of q. The plasmon frequency falls off when the effective wave vector deviates from the easy direction. The superlattice plasmon frequency tends to that of a single tubule when the plasmon wavelength is small compared to intertubule distance a ($aq >> 1$), and it converges to the plasmon frequency of the uniform electron gas when the wavelength is large compared to a ($aq << 1$). The lattice contribution to the plasmon frequency which is always negative due to the extra constraints imposed by the lattice structure, is most significant in the intermediate wavelengths.

As mentioned in the Introduction, in two recent papers by Lin *et al.* [15, 16] have calculated the plasmon frequencies for a three-dimensional carbon nanotube bundle. However, we believe that our calculation is different from theirs in several important respects. First, these authors do not consider a two-dimensional superlattice at all. So the calculation and results presented in Section 3 are all new. This case is important to study since such a system has been realized in practice. Second, from the calculation they presented we cannot be sure if they have carried out a lattice summation to include the hexagonal closed packed distribution of the individual nanotubes. Furthermore, they seem to use the three-dimensional form of the Coulomb potential for the interaction between electrons on different nanotubes, whereas we have used the more precise form of this interaction involving modified Bessel functions [see eq. (12)]. Perhaps for these reasons our results are different from theirs. While they do not consider the different directions of the Brillouin zone, they seem to incorporate direction dependence by the angle θ measured from the axis of aligned nanotubes. Such an angular dependence seems to miss variation of results in different directions of the Brillouin zone. This may be the reason as to why they missed the fact the plasmon frequency starts out being pseudo acoustic for small values q away from the Γ point.

Acknowledgments

This work has been partially supported by the NATO Research Grant No. CRG 910966. The work of P. L. has also been supported by the National Fund for Scientific Research (Belgium). We thank Joseph T. Schick who provided valuable help by plotting Figures 1 and 3 using our computed data.

References

[1] S Iijima *Nature* **354** 56 (1991)
[2] T W Ebbesen and P M Ajayan *Nature* **358** 220 (1992)
[3] P M Ajayan *et al Science* **265** 1212 (1994)
[4] W A de Heer *et al Science* **268** 45 (1995)
[5] A Thess *et al Science* **273** 483 (1996)
[6] W Z Li *et al Science* **274** 1701 (1996)
[7] M Terrones *et al Nature* **388** 52 (1997)
[8] F J Garcia-Vidal, J M Pitarke and J B Pendry *Phys Rev Lett* **78** 4289 (1997)
[9] R S Lee *et al Nature* **388** 255 (1997)
[10] W A de Heer, A Châtelain and D Ugarte, *Science* **270** 1179 (1995)
[11] G Baumgartner *et al Phys Rev* **B 55** 6704 (1997)
[12] O Chauvet *et al Phys. Rev* **B53** 13996 (1996)
[13] S M Bose and P Longe *J Phys : Cond Matter* **4** 1799 (1992)
[14] P Longe and S M Bose *Phys Rev* **B48** 18239 (1993)
[15] M F Lin, D S Chuu and K W -K Shung *Phys. Rev.* **B56** 1430 (1997)
[16] M F Lin and D S Chuu *Phys Rev* **B 57 10** 183 (1998)
[17] J Tersoff and R S Ruoff *Phys. Rev Lett.* **73** 676 (1994)